

1 ***Proteasome granular localization is regulated through***
2 ***mitochondrial respiration and kinase signaling***

3
4 Kenrick A Waite and Jeroen Roelofs[#]

5
6 Department of Biochemistry and Molecular Biology, University of Kansas Medical
7 Center, Kansas City, 3901 rainbow Blvd., HLSIC 1077, Kansas, USA

8 [#]correspondance: jroelofs@kumc.edu

9 **Running title:** Mitochondrial function regulates proteasome localization

10
11 **Keywords:** proteasome, liquid-liquid phase separation, mitochondrial respiration, MAP
12 kinases, proteasome storage granules (PSG), proteaphagy, mitochondrial inhibition,
13 autophagy.

14
15
16

17 **Summary**

18 We determined a role for mitochondrial respiration in regulating proteasome granule
19 formation and identified the cell integrity MAP kinase pathway and Snf1 kinase as
20 regulatory factors.

21

22 **Abstract**

23 In yeast, proteasomes are enriched in cell nuclei where they execute important cellular
24 functions. Nutrient-stress can change this localization indicating proteasomes respond to
25 the cell's metabolic state. However, the signals that connect these processes remain
26 poorly understood. Carbon starvation triggers a reversible translocation of proteasomes
27 to cytosolic condensates known as proteasome storage granules (PSGs). Surprisingly,
28 we observed strongly reduced PSG levels when cells had active cellular respiration prior
29 to starvation. This suggests the mitochondrial activity of cells is a determining factor in
30 the response of proteasomes to carbon starvation. Consistent with this, upon inhibition of
31 mitochondrial function we observed proteasomes relocate to granules. These links
32 between proteasomes and metabolism involve specific signaling pathways, as we
33 identified a MAP kinase cascade that is critical to the formation of proteasome granules
34 after respiratory growth but not following glycolytic growth. Furthermore, the yeast
35 homolog of AMP kinase, Snf1, is important for proteasome granule formation induced by
36 mitochondrial inhibitors, while dispensable for granule formation following carbon
37 starvation. We propose a model where mitochondrial activity promotes proteasome
38 nuclear localization.

39

40

41

42 **Introduction**

43 The efficiency of many cellular processes relies on optimal levels of the proteins
44 involved. To achieve this, there is a network of factors that coordinate protein synthesis,
45 folding, localization, and degradation, known as the proteostasis network. Protein
46 degradation is mainly controlled by two pathways in eukaryotes, the Ubiquitin-
47 Proteasome System (UPS), and the autophagy-lysosome pathway (Finley *et al.*, 2012;
48 Feng *et al.*, 2014; Dikic, 2017). Substrates of the UPS are labeled with one or more
49 ubiquitins in a highly selective process (Hershko and Ciechanover, 1998; Schrader,
50 Harstad and Matouschek, 2009; Finley *et al.*, 2012). In humans more than 600 ubiquitin
51 ligases are dedicated to the recognition and labeling of specific proteasome substrates
52 (Li *et al.*, 2008). While many ubiquitinated proteins are recognized and degraded by
53 proteasomes, ubiquitination also serves other functions depending on the type of
54 ubiquitination and cellular state (Fujii *et al.*, 2009; Shaid *et al.*, 2013; Rittinger and Ikeda,
55 2017). The second pathway of protein degradation is the autophagy-lysosome system.
56 Here, macro-autophagy, hereafter referred to as autophagy, is the major pathway.
57 Autophagy (literally self-eating) involves the targeting of proteins to the concave side of
58 de novo formed double membrane structures. Upon expansion and closure of these
59 structures, an autophagosome is formed that has engulfed cytosolic cargo (Kabeya *et al.*,
60 2000; Feng *et al.*, 2014; Dikic, 2017). Fusion of the outer membrane of these
61 autophagosomes with lysosome (vacuoles in yeast and plants) exposes the inner
62 membrane and engulfed material to acidic hydrolases that degrade the content.
63 Autophagy can be divided into selective and non-selective processes. These are
64 differentially regulated depending on the substrate and cellular conditions. While there is
65 overlap amongst proteasome and autophagy substrates, autophagy is uniquely capable
66 of clearing protein aggregates, damaged organelles, viruses, and large multi-subunit
67 complexes (Ogata *et al.*, 2006; Kraft, Reggiori and Peter, 2009; Kamada *et al.*, 2010;
68 Deffieu *et al.*, 2013; Marshall *et al.*, 2015; Mochida *et al.*, 2015; Waite *et al.*, 2015; BAO
69 *et al.*, 2016).

70 Proteasomes are one of the large multi-subunit complexes that are degraded via
71 autophagy, a process referred to as proteaphagy. Proteaphagy appears to be a selective
72 process as it depends on factors not involved in general autophagy (Waite *et al.*, 2015;

73 Cohen-Kaplan *et al.*, 2016; Marshall, McLoughlin and Vierstra, 2016; Nemeč *et al.*, 2017;
74 Li *et al.*, 2019) and does not occur under several conditions that induce general autophagy
75 (Waite *et al.*, 2021). A striking example of this is carbon starvation, which induces general
76 autophagy (Adachi, Koizumi and Ohsumi, 2017). Proteasomes, however, localize to
77 cytosolic punctate structures termed proteasome storage granules (PSGs) upon carbon
78 starvation (Laporte *et al.*, 2008). While several factors that regulate PSG formation or
79 their subsequent dissolution have been identified (Peters Lee Zeev *et al.*, 2013;
80 Weberruss *et al.*, 2013; van Deventer *et al.*, 2014; Marshall and Vierstra, 2018; Li *et al.*,
81 2019), the signals that trigger proteasome relocalization and the mechanisms that
82 regulate it have not been resolved.

83 Grown in the presence of glucose, yeast mainly utilize glycolysis for energy (ATP)
84 and biomass production, while suppressing mitochondrial respiration (Kayikci and
85 Nielsen, 2015). However, upon depletion of glucose, cells adapt and the metabolism
86 switches from mainly glycolysis to mitochondrial respiration. This process is facilitated by
87 autophagy, which provides a source of serine required for mitochondrial one-carbon
88 metabolism (May, Prescott and Ohsumi, 2020). While uniquely adapted to utilize glucose
89 as a carbon source, yeast grown in the presence of other carbon sources, like raffinose
90 or glycerol, primarily utilize mitochondrial respiration for energy production (Kayikci and
91 Nielsen, 2015; Adachi, Koizumi and Ohsumi, 2017). Interestingly, yeast do not induce
92 general autophagy when switched from glucose containing media to carbon starvation
93 media, presumably due to the lack of ATP. However, yeast grown on non-glucose carbon
94 sources prior to starvation do induce general autophagy upon removal of the carbon
95 source (Adachi, Koizumi and Ohsumi, 2017). This suggests the cellular respiratory state
96 and ATP levels are determinants in signaling autophagy. However, it should be noted that
97 the difference between glycolytic growth with repressed respiration and growth with active
98 mitochondrial respiration is also accompanied by a differences in the expression of
99 numerous genes (Galdieri *et al.*, 2010).

100 As proteasomes and autophagy both contribute to the replenishment of cellular
101 metabolites, we hypothesized that the metabolic state of cells, like with autophagy,
102 impacts proteasomes as well. Here, we report the relocalization of proteasomes to PSGs
103 is restricted when yeast are starved following respiratory growth, but not glycolytic growth

104 (where respiration is suppressed). Consistent with this, conditions that interfered with
105 mitochondrial function, such as inhibition of different electron transport chain complexes,
106 resulted in the formation of proteasome granules in yeast. This differential regulation
107 based on the initial carbon source involves specific signaling pathways: the AMP kinase
108 Snf1 and a MAP kinase signaling cascade, both regulate proteasome granule formation.
109 We propose a model where proteasome localization is regulated through mitochondrial
110 respiration.

111

112 **Results**

113

114 ***Proteasome Granule Formation is Restricted During Respiratory Growth.***

115 The observation that the growth media prior to carbon starvation influenced yeast's
116 autophagic response resolved a controversy regarding general autophagy induction
117 following carbon starvation (Takeshige *et al.*, 1992; Lang *et al.*, 2014). Starvation
118 following respiratory growth (like in media containing raffinose or glycerol as the carbon
119 source), promoted autophagy induction while growth in glycolytic/fermenting media, like
120 dextrose (D-glucose), did not (Adachi, Koizumi and Ohsumi, 2017). Consistent with this,
121 a link between respiration and autophagy induction during energy deprivation has been
122 established (Yi *et al.*, 2017). Thus, the metabolic state of the cell is an important variable
123 when evaluating carbon starvation responses. We previously showed that carbon
124 starvation does not induce proteasome autophagy in yeast (Waite *et al.*, 2016), however
125 we did not specifically control for the pre-starvation condition of the cells. Therefore, we
126 used media containing dextrose (YPD, glycolysis), raffinose (YPR, glycolysis and
127 respiration), or glycerol (YPG, respiration exclusively) as sources of carbon to examine
128 proteaphagy following carbon starvation. We monitored proteasome autophagy with a
129 GFP-tag fused to the regulatory particle subunit Rpn1. Here, the observation of vacuolar
130 fluorescence in cells or the appearance of a faster migrating “free” GFP species on
131 immunoblots are indicative of proteaphagy. No robust proteaphagy was observed upon
132 switching to carbon starvation, independent of the growth medium prior to starvation. The
133 amount of “free” GFP detected at 1 and 2 days of carbon starvation was less than “free”
134 GFP detected following six hours of nitrogen starvation (Waite *et al.*, 2015) (Fig. 1A).

135 Instead, proteasome granules were induced, as previously reported (Waite *et al.*, 2015;
136 Marshall and Vierstra, 2018). Interestingly, pre-growth in dextrose resulted in
137 approximately 58% of cells showing granules with 27% of these showing multiple
138 granules per cell, whereas pre-growth in raffinose resulted in less than 32% of cells
139 showing granules and 5% of these showing multiple granules per cell (Fig. 1B). A similar
140 trend was observed when we monitored the core particle using α 1-GFP as a reporter
141 (S1). This suggest that proteasome localization is affected by the carbon source cells
142 were grown in prior to starvation.

143 To explore the role of nutrients in proteasome localization further, we analyzed the
144 induction of PSGs following prolonged growth in rich media, another condition that results
145 in PSG formation (Laporte *et al.*, 2008; Peters *et al.*, 2016). When granules formed after
146 growth for an extended period, a single dominant granule was observed in cells
147 regardless of the initial carbon source. However, we observed that cells grown in rich
148 media containing dextrose for 3 days had more cells forming granules in general than
149 cells grown in media containing raffinose. Growth in glycerol media resulted in very few
150 cells forming granules after 3 days (Fig. 1C). This was also observed with α 1-GFP as a
151 reporter (S2). Consistent with a model where PSGs protect proteasomes from autophagy
152 (Marshall and Vierstra, 2018), the conditions with less granules (i.e. raffinose and
153 glycerol) showed more “free” GFP on immunoblots at both 2 and 3 days of growth in
154 carbon containing media, (Fig. 1C, S3) suggesting an increase in proteaphagy. However,
155 we would expect more proteaphagy following growth in glycerol considering this condition
156 formed markedly fewer PSGs (Fig. 1C). Interestingly, we observed GFP-positive bands
157 on immunoblots with molecular weights between “free GFP” and Rpn1-GFP following
158 prolonged growth in glycerol. Such fragmentation patterns were recently observed
159 specifically for GFP-tagged proteasomes degraded through ESCRT-mediated micro-
160 autophagy (Li *et al.*, 2019). In all, our data suggest that not only PSGs, but also the type
161 and magnitude of proteasome autophagy, is dependent on the initial carbon source and
162 the cell’s metabolic state prior to starvation.

163 Switching from dextrose media to carbon starvation results in the formation of
164 multiple phagophore assembly sites (PAS), which does not occur when carbon starvation
165 is initiated following prior growth in other carbon sources or upon nitrogen starvation. This

166 likely affects autophagy induction and might contribute to the lack of autophagy in this
167 condition (Adachi, Koizumi and Ohsumi, 2017). The number of proteasome granules
168 observed per cell correlates with increased PAS sites when comparing switching from
169 dextrose or raffinose to carbon starvation (Fig. 1B, S1). To determine if proteasomes co-
170 localized with PAS during carbon starvation, we used cells expressing GFP-Atg8 (PAS/
171 autophagy marker) and Rpn1-mCherry. We monitored GFP and mCherry localization
172 upon carbon starvation after pre-growth in dextrose, raffinose, or glycerol containing
173 media (Fig. 1D). PAS structures were observed within 1 hour of starvation, when no PSGs
174 are yet detectable. At 24 hours when both PSG and PAS can be observed, we did not
175 observe any striking colocalization (Fig. 1D), indicating these are distinct structures. To
176 test if PSG formation depended on PAS formation or the signaling pathway that induces
177 an autophagic response upon carbon starvation, we analyzed strains deleted for different
178 genes required for autophagy induction: ATG1, SNF1 and GGC1. These gene products
179 activate Mec1 in a process that tethers Mec1 to the mitochondrial outer membrane upon
180 carbon starvation. This mitochondrial localization together with active mitochondrial
181 respiration are prerequisites for autophagy induction (Yi *et al.*, 2017). ATG1, SNF1, and
182 GGC1 were not required for proteasome granule formation upon carbon starvation (S4)
183 indicating multiple distinct signals couple the cells metabolic state to these two
184 degradative machineries. The majority of cells formed PSGs at 24 hours when pre-grown
185 in dextrose (~56%), which was significantly higher compared to cells pre-grown in
186 raffinose or glycerol (26% and 22% respectively) (Fig. 1D). In sum, conditions where cells
187 initially had active respiration show less PSGs.

188 To further probe the role of mitochondrial respiration in regulating proteasome
189 localization, we tested other conditions that induce respiration vs glycolysis. First, we
190 tested the carbon starvation response after growing cells for 4 hours (more glycolysis and
191 fermentation) or 24 hours (more respiration) in YPD medium. After 24 hours of dextrose
192 depletion, yeast have switched to respiration for energy production (Galdieri *et al.*, 2010).
193 Indeed, starving after 24 hours of growth in dextrose resulted in a reduction in granule
194 formation compared to 4 hours (S5). Next, we starved cells for phosphate following
195 growth in different carbon sources. This was based on the rationale that cells lacking
196 phosphate sources would be compromised in maintaining energy production as

197 phosphate is required for ATP production (Ko, Hong and Pedersen, 1999). Phosphate
198 starvation induces cell cycle arrest and a stress response similar to carbon starvation
199 (Petti *et al.*, 2011; Secco *et al.*, 2012). Phosphate starvation also induced proteasome
200 autophagy but to a lesser extent than nitrogen starvation at 24 hours (Waite *et al.*, 2021).
201 Here, we show that prolonged phosphate starvation induced proteasome granules
202 (Fig.1E). Like PSGs induced by carbon starvation, these granules had different properties
203 depending on the initial carbon source. Cells grown in raffinose that were starved for
204 phosphate showed less PSGs compared to cells grown in dextrose. Even more striking
205 was the almost complete absence of granules when cells were grown in glycerol (Fig.
206 1E), even though our phosphate starvation media always contained dextrose as a carbon
207 source. Catabolite repression does not appear to play a role here as raffinose and glycerol
208 pre-growth resulted in distinct phenotypes. Because granules induced by phosphate
209 starvation are evident only at later timepoints (2 days), they could result from prolonged
210 growth similar to granules formed during stationary phase. However, we found granules
211 were induced to a much larger extent in SD media lacking phosphate compared to SD
212 complete media, both of which contained dextrose as a carbon source (S6). In all,
213 proteasome granule formation appears to be in part dependent on mitochondrial
214 respiration. Under conditions of limited mitochondrial respiration, proteasomes appear to
215 re-localize to PSGs more efficiently.

216

217 ***Mitochondrial Inhibition Induces Proteasome Granule Formation***

218 Cells grown in respiratory media formed fewer PSGs when starved for carbon,
219 phosphate, or grown for three days. Thus, increased mitochondrial function appears to
220 limit PSG formation. This led to the hypothesis that reducing mitochondrial function has
221 opposing effect and causes proteasome granule formation. To test this, we inhibited
222 mitochondrial function by targeting different components of the electron transport chain
223 (ETC). Sodium azide, antimycin A, and oligomycin A were used to target complex IV,
224 complex III, and ATP synthase respectively. We further utilized the uncoupler CCCP to
225 disrupt ATP synthesis (Heytler and Prichard, 1962; Wikström and Berden, 1972; Gribble
226 *et al.*, 1997; Symersky *et al.*, 2012). All four drugs induced proteasome granules in rich
227 (dextrose) media (Fig. 2A), further corroborating the link between mitochondrial function

228 and proteasome localization. To test if granules induced through mitochondrial inhibition
229 behave like proteasome granules induced by carbon starvation, we tested the reversibility
230 of these granules. Carbon starvation induced PSGs, unlike other types of proteasome
231 containing granules, quickly disappear with proteasomes re-localizing to cell nuclei upon
232 re-addition of a carbon source (Laporte *et al.*, 2008; Peters Lee Zeev *et al.*, 2013;
233 Weberruss *et al.*, 2013; Waite, Burris and Roelofs, 2020). Granules induced by
234 mitochondria inhibitors quickly dissipated and GFP signal was predominantly nuclear
235 after cells were washed and re-inoculated into drug free media (Fig. 2B, S7). This
236 indicates that these granules are not associated with irreversible aggregates but are
237 dynamic structures consistent with the proposed storage function of PSGs. Similar to ETC
238 inhibitors, we predicted the absence of the final electron acceptor, oxygen, should also
239 result in PSG formation by inhibiting oxidative phosphorylation. Indeed, upon growth in
240 anoxic conditions, proteasome granules were induced (S8). Like with carbon starvation,
241 the magnitude of mitochondria inhibition-induced granules was dependent on the carbon
242 source during initial growth with the exception of Rpn1-GFP cells treated with antimycin
243 A (Fig. 2C). These data further indicate a role for mitochondrial respiration in regulating
244 proteasome granule formation.

245 Intriguingly, we did not detect induction of proteasome granules with all
246 mitochondria inhibitors tested. Surprisingly, potassium cyanide (KCN) treatment, which
247 like azide targets cytochrome c oxidase, did not result in any significant granule formation
248 at various concentrations (Fig. 2D). The KCN treated cells grew slower than untreated
249 cells (with a growth rate comparable to other mitochondria inhibitors) and we observed
250 an increase in cell size at high concentrations (Fig. 2D), indicating KCN treatment was
251 effective. Apparently mitochondrial inhibition or stress alone is not sufficient for PSG
252 formation.

253 Mitochondria play a key role in efficient ATP production and ATP is essential for
254 proteasome function (Finley, 2009; Schrader, Harstad and Matouschek, 2009).
255 Furthermore, proteasome complexes are unstable *in vitro* in the absence of ATP (Kleijnen
256 *et al.*, 2007). Therefore we wondered if ATP maintenance and proteasome stability are
257 key determinants in PSG formation; something that has been postulated before (Enenkel,
258 2018; Karmon and Ben Aroya, 2020). To test if PSG formation was linked to ATP

259 production, we measured ATP under PSG inducing and non-inducing stimuli. To do this,
260 we utilized the Cell Titer Glo as well as the Enliten ATP assay systems (Nicastro *et al.*,
261 2015; Adachi, Koizumi and Ohsumi, 2017). Inhibiting mitochondria with sodium azide,
262 antimycin A, oligomycin A, CCCP and growing yeast anoxically, led to a large reduction
263 in ATP compared to growth in rich media (Fig. 2E). This reduction in ATP levels correlated
264 with PSG formation (Fig. 2E). Interestingly, KCN treatment caused a smaller reduction in
265 ATP levels compared to the untreated control, and this inhibitor did not induce PSGs.

266 We next measured ATP under starvation conditions. We observed a larger
267 reduction in ATP following nitrogen starvation than carbon starvation, while only carbon
268 starvation induced granule formation. Similarly, we observed a strong reduction in ATP
269 detected following 24 hours of phosphate starvation, a condition that induces proteasome
270 autophagy with PSGs observed 48 hours post starvation (Fig. 1F) (Waite *et al.*,
271 2021). Thus, with starvation, a reduction in ATP levels by itself does not trigger
272 proteasomes re-localization to PSGs. One possible explanation is that in addition to a
273 drop in ATP levels, other signals are generated during nitrogen and phosphate starvation
274 that result in proteaphagy.

275

276 ***MAP Kinase Signaling is Required for Proteasome Granule Formation***

277 The differential regulation of proteasome granules observed following respiratory
278 vs non-respiratory growth, as well as the observation that not all mitochondria inhibitors
279 induce proteasome granules (Fig. 2D), suggests that there is some regulator of this
280 process that is only active under specific conditions. The cell wall integrity MAP kinase
281 cascade proteins Mpk1(Slt2), Mkk1, and Mkk2 are known to regulate proteasome
282 abundance and proteasome autophagy (Rousseau and Bertolotti, 2016; Waite *et al.*,
283 2021). This kinase cascade has further been shown to be required for induction of general
284 autophagy when antimycin A or potassium cyanide were added to cells in a process that
285 was dependent on Atg32 and Atg11 (Deffieu *et al.*, 2013). When we tested if deletion of
286 *ATG32* disrupted the formation of proteasome granules induced after prolonged yeast
287 growth, azide or antimycin A treatment, we observed no reduction in PSG formation (S9).
288 Similarly, *ATG11* was not required for granule formation when cells were treated with
289 sodium azide (S10). This shows that the requirements for autophagy induction and PSG

290 formation are not identical in these conditions. Next, we wanted to test the role of MAP
291 kinase signaling itself. To test if the MAPK Mpk1 was important for PSG formation, we
292 deleted the MPK1 gene. In these cells we observed a striking difference depending on
293 the initial carbon source used. PSG formation was unaffected in a *mpk1* Δ strain when
294 starved for carbon following initial growth in dextrose (Fig. 3A, E). However, when yeast
295 were grown in raffinose prior to starvation, Mpk1 was critical to form granules efficiently
296 for both the RP (Rpn1) and CP (α 1) reporters (Fig. 3A, E). This suggest that Mpk1 was
297 required for proteasome granule formation in cells that had active mitochondrial
298 respiration. When we monitored granule formation following oligomycin A, antimycin A
299 and CCCP treatment, we found a similar requirement for Mpk1 when cells were grown in
300 raffinose (Fig. 3B-D, F). With respect to sodium azide, granules monitored using a GFP-
301 tag on the CP subunit α 1 behaved as above with a reduction in the MPK1 mutant following
302 growth in raffinose (Fig. 3E, F). Granule formation monitored using GFP-tag on the RP
303 subunit Rpn1 , however, was restricted when *mpk1* Δ cells were grown in dextrose but
304 not raffinose (Fig. 3E, F). This observation further supports the idea of differential
305 regulation of CP and RP in granule formation, as has been observed before (Weberruss
306 *et al.*, 2013; Marshall and Vierstra, 2018; Karmon and Ben Aroya, 2020). Next, we tested
307 for a role of the proteasome chaperone Adc17. Adc17 is activated under several stress
308 conditions (Hanssum *et al.*, 2014) by Mpk1 (Rousseau and Bertolotti, 2016). However,
309 Adc17 was dispensable for PSG formation, suggesting an alternate route of proteasome
310 regulation by Mpk1(S11).

311 To determine the involvement of other kinases, we analyzed a number of proteins
312 within the cell integrity pathway, as well as other major yeast MAPKs from independent
313 pathways (Levin, 2005). The deletion of *FUS3* or *HOG1* (MAPKs involved in pheromone
314 response and osmoregulation respectively) did not prevent or substantially reduce
315 proteasome granule formation (S11). This indicates a specific role for the cell integrity
316 kinase pathway. Looking at MAP kinase kinases upstream of Mpk1, we evaluated Mkk1
317 and Mkk2. While individual deletion of these paralogs had little impact on granule
318 formation, a double deletion of *MKK1* and *MKK2* showed only few proteasome granules
319 under carbon starvation, azide treatment, antimycin A, oligomycin A and CCCP treatment
320 (Fig. 3F). This reduction was, like with Mpk1, observed when cells were grown in raffinose

321 but not glucose prior to treatment. Tracing this MAP kinase cascade further, we found
322 that the MAPKKK Bck1 was similarly required, however these cells formed more granules
323 after switching from glucose media than MPK1 or MKK1/MKK2 mutants. Though we did
324 observe a more significant reduction compared to wildtype when cells were cultured in
325 raffinose (Fig. 3G). Upstream of Bck1, the transmembrane activator of the cascade,
326 Wsc1, was also required for granule formation (S12). Other upstream activators of the
327 cell integrity pathway, namely Wsc2, Wsc3 and Ack1 (Verna *et al.*, 1997; Kuranda *et al.*,
328 2006; Krause, Xu and Gray, 2008), were not required for PSG formation under the same
329 conditions (S12). Our data show that an intact map kinase pathway, starting at Wsc1 and
330 moving downstream to Mpk1, is required for proteasome granule formation when cells
331 are grown in respiration inducing conditions. We have previously reported that Mpk1,
332 Mkk1 and Mkk2 are required for efficient proteaphagy (Waite *et al.*, 2021). Both conditions
333 require nuclear export of proteasomes, potentially indicating this kinase cascade
334 regulates nuclear export of proteasomes, for example by Mpk1 directly phosphorylating
335 proteasomes. However, Mpk1 is involved in many cellular processes and this kinase
336 pathway might be indirectly involved in signaling proteasome re-localization. These
337 possibilities are currently being tested.

338

339 ***Snf1 is required for proteasome granule formation upon mitochondrial inhibition***

340 As mentioned above, Snf1 is required for the induction of autophagy upon glucose
341 starvation. This kinase is recruited to mitochondria shortly after the onset of glucose
342 starvation where it phosphorylates Mec1. Phosphorylated Mec1 recruits Atg1 to
343 mitochondria and both factors are required for maintaining mitochondrial respiration
344 during glucose starvation (Yi *et al.*, 2017). This respiration in turn is also required for
345 autophagy induction (Adachi, Koizumi and Ohsumi, 2017; Yi *et al.*, 2017). We did not
346 observe a reduction in PSGs upon carbon starvation when SNF1 or other factors involved
347 in this pathway were deleted (S4), a finding consistent with published data (Li *et al.*, 2019).
348 Snf1 was also not required for proteasome autophagy induced by nitrogen starvation, but
349 was required for proteasome autophagy observed following 4 days of growth in SC media
350 with 0.025% (low) glucose (Li *et al.*, 2019). Intriguingly, we noticed a different role for Snf1
351 in proteasome autophagy under growth with different carbon sources. Deletion of SNF1

352 promoted autophagy of proteasomes when cells were grown for 3 days in rich media
353 containing dextrose or glycerol but not raffinose (Fig. 4A). Further, we observed that
354 SNF1 mutants failed to form proteasome granules efficiently under these conditions (Fig.
355 4B). This is consistent with a model whereby PSGs protect proteasome from autophagic
356 degradation (Marshall and Vierstra, 2018), however, we did not observe increased
357 autophagy when cells were grown in raffinose, despite the failure in granule formation in
358 this condition. Here, GFP signal appeared more nuclear and diffuse in the cytoplasm for
359 the Snf1 mutant than the wildtype which formed PSGs (Fig. 4B). The disparate
360 phenotypes we observed likely reflect the complexity of combined inputs to cells
361 metabolic state and mitochondrial respiration activity in regulating proteasome
362 localization.

363 To gain more insight into the role of Snf1 in regulating proteasomes localization,
364 autophagy, and granule formation, we tested the effect of mitochondria inhibitors in these
365 cells. Unlike granules induced by carbon starvation, granules induced with mitochondria
366 inhibitors were highly dependent of Snf1 (Fig. 4C) for both the RP and CP tag reporters
367 (Li *et al.*, 2019). Upon mitochondrial inhibition, compared to wild type, Snf1 mutants have
368 fewer proteasome granules, more nuclear GFP signal and little to no vacuolar GFP signal.
369 Of note, these cells were grown in glucose where Snf1 is inactive (Schüller, 2003; Kayikci
370 and Nielsen, 2015). This may indicate an alternative role for Snf1 in regulating
371 proteasome localization outside of its canonical role of non-fermentative gene repression.
372 In all, these data suggest that different pathways are involved in the formation of
373 proteasome storage granules, for example during carbon starvation versus mitochondria
374 inhibition. This raises the question to what extent these granules are similar or
375 qualitatively different in function or regulation.

376

377 ***Discussion***

378 The transcriptional upregulation of proteasomes (by Rpn4 in yeast and Nrf1 in
379 mammals) is critical for cells to respond to various stress conditions. However, not all
380 stresses require a (continuous) upregulation of proteasomes and instead trigger either
381 the degradation of proteasomes or their relocalization into cytosolic granules. In yeast,
382 proteasome complexes are enriched in the nucleus under optimal conditions such as

383 during logarithmic growth. However, proteasomes re-localize to cytoplasmic granules
384 upon carbon limitation (Enenkel, 2012; Peters Lee Zeev *et al.*, 2013; Waite *et al.*, 2015;
385 Marshall and Vierstra, 2018). When stressed for nitrogen, on the other hand, proteaphagy
386 is induced (Marshall *et al.*, 2015; Waite *et al.*, 2015; Nemeč *et al.*, 2017). Similarly, in
387 human cells, proteasomes have been reported to undergo proteaphagy in response to
388 amino acid starvation or upon proteasome inhibition (Cohen-Kaplan *et al.*, 2016; Choi *et al.*
389 *et al.*, 2020; Goebel *et al.*, 2020). Interestingly, cytoplasmic proteasomes appear to be
390 substrates for proteaphagy upon amino acid deprivation while nuclear proteasomes
391 undergo liquid-liquid phase separation (LLPS) (Uriarte *et al.*, 2021). Osmotic stress has
392 also been shown to induce nuclear LLPS granules of proteasomes (Yasuda *et al.*, 2020).
393 Thus, both in yeast and humans depending on the condition, proteasomes show distinct
394 fates and localization. To understand how these specific fates of proteasomes are
395 regulated, we need to not only know the factors involved, but also understand the triggers
396 responsible. This can be rather subtle, as it was recently shown that clearly defined fates
397 for proteasomes were observed when comparing cells starved with low levels of glucose
398 or no glucose at all (Li *et al.*, 2019). Here, only the cells starved in low glucose induced
399 Snf1-dependent micro-autophagy of proteasomes. In the current study, we sought to
400 determine in detail what triggers proteasome granular localization and further identified
401 some of the key signaling kinases involved.

402

403 **Mitochondrial Respiration as key determinant.**

404 Our data show that mitochondrial respiration, at least in part, regulates proteasome
405 localization (Figs. 2, 5). First, we show that several inhibitors of mitochondrial respiration
406 robustly induce PSG formation. Second, removing a carbon source from cells that grew
407 in media that suppresses respiration (i.e. with glucose (Galdieri *et al.*, 2010)) resulted in
408 the formation of multiple granules per cell, whereas one dominant granule was present
409 when cells were switched from media that required respiration (glycerol or raffinose). This
410 observation shows interesting parallels with the regulation of general autophagy upon
411 carbon starvation that was recently shown to be dependent on respiration (Adachi,
412 Koizumi and Ohsumi, 2017). Another study found a complex of Snf1-Mec1-Atg1 is
413 recruited to the mitochondrial membrane by Ggc1 following the onset of carbon

414 starvation. The formation of this complex is required to maintain active mitochondrial
415 respiration which in turn is required to initiate carbon starvation induced autophagy (Yi *et*
416 *al.*, 2017). Surprisingly, the deletion of GGC1 did not impact PSG formation, suggesting
417 additional signaling pathways link respiration to the regulation of proteasome localization.

418 The extent of granule formation when cells were grown in different carbon sources
419 negatively correlated with the amount of general autophagy induced , as we detected a
420 reduction in the number of PSGs under conditions that led to increased general
421 autophagy upon carbon starvation (Adachi, Koizumi and Ohsumi, 2017). Here, we
422 observed only a small increase in proteaphagy (Fig. 1A) when cells were grown in
423 respiratory media, suggesting the reduced levels of PSGs cannot be explained by
424 increased autophagy of proteasomes. This is in contrast to the reported role of PSGs in
425 protecting proteasomes from autophagy as we would expect more proteasome
426 autophagy when there is a reduction in PSGs. Our data suggest that proteasomes are
427 excluded from autophagic degradation without being sequestered into PSGs. This may
428 indicate a role for proteasome activity in regulating the autophagic response of respiring
429 cells. Further supporting our observations is the lack of an increase in proteasome
430 autophagy under autophagic conditions in mutants that are defective in granule formation
431 (Figs. 3 and 4). The nuclear enrichment of fluorescence we observed under these
432 conditions indicates that the majority of proteasomes remained nuclear. This localization
433 shields proteasomes from general autophagy (Waite *et al.*, 2015; Nemeč *et al.*, 2017).
434 Thus, proteasomes can be excluded from autophagic degradation either by PSG
435 formation or by nuclear retention. In line with this, the deletion of autophagy related genes
436 results in nuclear retention (Waite *et al.*, 2015, 2021) This suggest proteasome
437 relocalization is tightly regulated and below we discuss a kinase cascade we have
438 identified that is involved in this process.

439

440 **Kinases that regulate proteasome localization.**

441 MAP kinases and Snf1 signaling pathways both regulate proteasome localization,
442 however, each under distinct conditions. The Mpk1 kinase cascade was required
443 following growth in media that induced respiration, while Snf1 was required upon
444 mitochondrial inhibition (but not carbon starvation). These pathways are known to

445 cooperate upon cell wall and oxidative stress (Backhaus *et al.*, 2013; Willis *et al.*, 2018),
446 indicating they might work together to regulate proteasomes more generally. Indeed, both
447 pathways are also involved in regulating proteasome abundance and mobilization upon
448 different stressors. Mpk1 is required for proteasome upregulation upon ER stress
449 (Rousseau and Bertolotti, 2016; Schmidt *et al.*, 2019) as well as required for efficient
450 proteaphagy (Waite *et al.*, 2021), and Snf1 is required for micro-autophagy of
451 proteasomes following growth in low glucose media (Li *et al.*, 2019). The requirement for
452 these pathways in both proteasome autophagy and proteasome granule formation could
453 indicate they are necessary for efficient nuclear export of proteasomes, a pre-requisite
454 for both autophagy and granule formation (Nemec *et al.*, 2017). However, the possibility
455 that they play a less direct role in regulating proteasome localization cannot be excluded.
456 It has been shown that MPK1 is required for general autophagy induction when
457 mitochondria are inhibited with the drug antimycin A (Deffieu *et al.*, 2013). Similarly, it is
458 required for mitophagy and pexophagy induced following nitrogen starvation, even though
459 general autophagy does not depend on Mpk1 (Mao *et al.*, 2011). Mitophagy here was
460 shown to depend on the complete the cell integrity MAPK cascade (from the
461 transmembrane receptor kinase Wsc1 to Mpk1). We demonstrate that this same cascade
462 is required for proteasome granule formation. These data point to a more general
463 signaling role for MPK1, particularly when mitochondria are affected. However, other
464 factors that are required for mitophagy under this conditions, such as Atg32, and Atg11,
465 had no effect on the formation of proteasome granules, suggesting that a general failure
466 in mitophagy does not correlate with a failure in proteasome granule formation.
467 Nevertheless, the MPK1 kinase cascade is clearly important in regulating proteasome
468 localization, particularly following respiratory growth.

469 An intact MAP kinase cascade is not sufficient to promote proteasome granule
470 formation. We report here that deletion of SNF1 restricted proteasome granule formation
471 upon inhibition of mitochondria. It was previously shown that this kinase is not required
472 for granule formation when cells were starved for glucose (Li *et al.*, 2019). The
473 requirement for this protein in these different context suggests that proteasome granules
474 induced upon carbon starvation versus mitochondrial inhibition are distinct. It is intriguing
475 that Snf1 was required for granule formation when cells were grown in glucose rich media,

476 as this protein is known to be inactive in this condition (Schüller, 2003; Turcotte *et al.*,
477 2010). This suggests an unidentified role for Snf1 in this context that regulates
478 proteasome localization.

479 In all our data show that proteasomes are specifically regulated under different
480 metabolic conditions. This may indicate that proteasome activity is similarly regulated
481 based on cellular needs. Given that the majority of proteasomes are nuclear, proteasome
482 capacity and activity must be altered when they re-localize. Indeed, the current literature
483 suggests that proteasomes are inactive in PSGs (Gu *et al.*, 2017; Enenkel, 2018).
484 Although it should be noted that LLPS structures induced by osmotic stress in HCT116
485 colon cancer cell line appear to be actively degrading ribosomal proteins (Yasuda *et al.*,
486 2020). Under conditions of mitochondrial respiration where proteasomes are more
487 nuclear, proteasome activity may be necessary. This observed relationship between
488 mitochondrial respiration and proteasome localization is intriguing, as other studies have
489 demonstrated a functional link between mitochondria and proteasomes (Bragoszewski *et*
490 *al.*, 2013; Bragoszewski, Turek and Chacinska, 2017; Lavie *et al.*, 2018). This is also
491 evident in Parkinson's disease where proteasomes play a crucial role in regulating
492 mitochondrial dynamics (Junn *et al.*, 2002; Ciechanover and Brundin, 2003; Webb *et al.*,
493 2003; Um *et al.*, 2010). Further, proteasomes are required to resolve mitochondrial stress
494 induced upon transporter clogging or accumulation of misfolded mitochondrial proteins in
495 the cytoplasm (Boos *et al.*, 2019). Our data show that proteasomes are responsive to
496 cellular metabolism and are regulated differently depending on the cell's metabolic status.
497 While ATP appears to not be the trigger for PSG formation, at least upon starvation, our
498 data make it clear that mitochondrial function and signaling play an important role.

499

500

501

502 **Materials and Methods**

503 **Yeast Strains**

504 All strains used in this study are reported in table S1. Our background strains are the
505 W303 derived SUB61 (*Mat α , lys2-801 leu2-3, 2-112 ura3-52 his3- Δ 200 trp1-1*) that arose
506 from a dissection of DF5 (Finley, Özkaynak and Varshavsky, 1987). Standard PCR based
507 procedures (primers and plasmids presented in table S2) were used to delete specific
508 genes from the genome, or introduce sequences at the endogenous locus that resulted
509 in the expression of C-terminal fusions of GFP or mCherry (Goldstein and McCusker,
510 1999; Hailey, Davis and Muller, 2002; Janke *et al.*, 2004).

511

512 **Yeast Growth Conditions**

513 Overnight cultures of yeast were inoculated at an OD₆₀₀ of 0.5 and grown in yeast extract
514 peptone (YEP) medium supplemented with 2% dextrose, raffinose or glycerol as a carbon
515 source and grown to an OD₆₀₀ 1.5 (approximately 4 hours). To induce starvation, cultures
516 growing logarithmically were centrifuged, washed with respective starvation medium, re-
517 inoculated at an OD₆₀₀ of 1.5, and incubated at 30 °C with constant shaking. Yeast
518 nitrogen base lacking carbon or phosphate sources was used to make the respective
519 starvation media. For drug treatments, cultures were grown to an OD₆₀₀ of 1.5 as above,
520 then treated. Sodium azide (VWR), antimycin A (Sigma), oligomycin A (Cayman
521 Chemical) and 2-[2-(3-chlorophenyl)hydrazinylidene]-propanedinitrile (CCCP) (Sigma),
522 were used at final concentrations of 0.5 μ M, 0.1 mM, 2.5 μ M and 10 μ M respectively.
523 Potassium cyanide (Fisher) was used at concentrations shown in Fig. 2E. Anoxic growth
524 was performed by transferring 1.8mL of logarithmically growing culture to a 2 mL culture
525 tube that was sealed and incubated without shaking for 24 hours at 30 °C.

526

527 **Protein Lysates and Electrophoresis**

528 For western blots, 2 ODs of cells were collected at indicated timepoints and treatments
529 and stored at -80 °C. Lysis was completed using previously establish methods
530 (Kushnirov, 2000). Following electrophoreses, samples were transferred to PVDF
531 membranes and immuno-blotted for GFP then Pgk1 followed by the appropriate
532 horseradish-peroxidase conjugated secondary antibodies. Antibodies used were anti-

533 GFP (1:500; Roche, #11814460001), and anti-Pgk1 (1:10,000; Invitrogen, #459250).
534 Horseradish-peroxidase activity was visualized using the Immobilon Forte Western HRP
535 substrate (Millipore), and images were acquired using the G-box imaging system
536 (Syngene) with GeneSnap software. Genetools was used to quantify the amount of free
537 GFP normalized to the Pgk1 loading control.

538

539 ***ATP Measurements***

540 Enliten ATP assay: 1 OD of cells was collected following indicated treatments and frozen
541 in liquid nitrogen. Pellets were resuspended in 50 μ L of 2.5% trichloro-acetic-acid (TCA)
542 and boiled for 3 mins. Sample was centrifuged (13,000 RPM) for 1 min and 2 μ L
543 supernatant was added to 98 μ L of 25 mM Tris-HCL [pH 8.8] (1:50 dilution). 10 μ L of 1:50
544 dilution was combined with 40 μ L of 25 mM Tris-HCL [pH 8.8] in a white 96 well plate. 50
545 μ L of rLuciferase/Luciferin reagent (Promega, ENLITEN® ATP Assay System) was added
546 to each well and luminescence was monitored using a plate reader.

547 Cell Titer Glo ATP assay: 0.5 OD of cells were centrifuged following indicated
548 treatments and resuspended in 50 μ L of sterile water. Samples were transferred to a 96
549 well black plate and 50 μ L of Cell Titer Glo 2.0® reagent was added. This plate was
550 incubated in the dark under constant rotation on an orbital shaker for 4 minutes. Following
551 rotation, the plate was further incubated in the dark for 10 minutes at room temperature.
552 Luminescence was then measured using a plate reader.

553

554 ***Fluorescence Microscopy***

555 All microscopy was performed with live yeast where proteasome subunits Rpn1 or α 1
556 was C-terminally tagged at their endogenous locus with expression driven by the
557 endogenous promoter. GFP-Atg8 was produced as previously described (Li *et al.*, 2015).
558 After indicated treatments, approximately 2 ODs of cells were pelleted, washed with PBS,
559 then resuspend in 30 μ L of PBS. 3 μ L of this sample was then mounted on 1% soft agar
560 slides as described by E. Muller (<https://www.youtube.com/watch?v=ZrZVbFg9NE8>)
561 (Sundin *et al.*, 2004). All imaging by fluorescence microscopy was done within 10 mins
562 following wash to avoid the effects of prolonged incubation on slides. Images were
563 acquired at room temperature using a Nikon Eclipse TE2000-S microscope at 600X

564 magnification with a Plan Apo 60x/1.40 objective equipped with a Retiga R3tm camera
565 (QImaging). Images were collected using Metamorph software (Molecular Devices) and
566 analyzed using FIJI. All quantification was performed using FIJI.

567

568 ***Acknowledgements***

569 We thank Dr. Stella Lee for helpful discussions and feedback on the manuscript. We
570 thank Mandeep Kaur for the generation of some of the yeast strains used in this study
571 and feedback on the manuscript. We thank Dr. Alicia Burris for sharing her observation
572 of proteasome granule formation under hypoxic conditions.

573

574 ***Competing interests***

575 The authors declare no competing or financial interests.

576

577 ***Author contributions***

578 Conceptualization: K.A.W., J.R.; Methodology: K.A.W., J.R.; Validation: K.A.W., J.R.;
579 Formal analysis: K.A.W., J.R.; Investigation: K.A.W.; Writing - original draft: K.A.W.;
580 Writing - review & editing: K.A.W., J.R.; Visualization: K.A.W., J.R.; Funding acquisition:
581 J.R.

582

583 ***Funding***

584 This work was supported by grants from the National Institutes of Health and National
585 Institute of General Medical Science (K-INBRE program P20GM103418 and
586 R01GM118660 to J. R.). The content is solely the responsibility of the authors and does
587 not necessarily represent the official views of the National Institutes of Health.

588

589 ***Supplementary information***

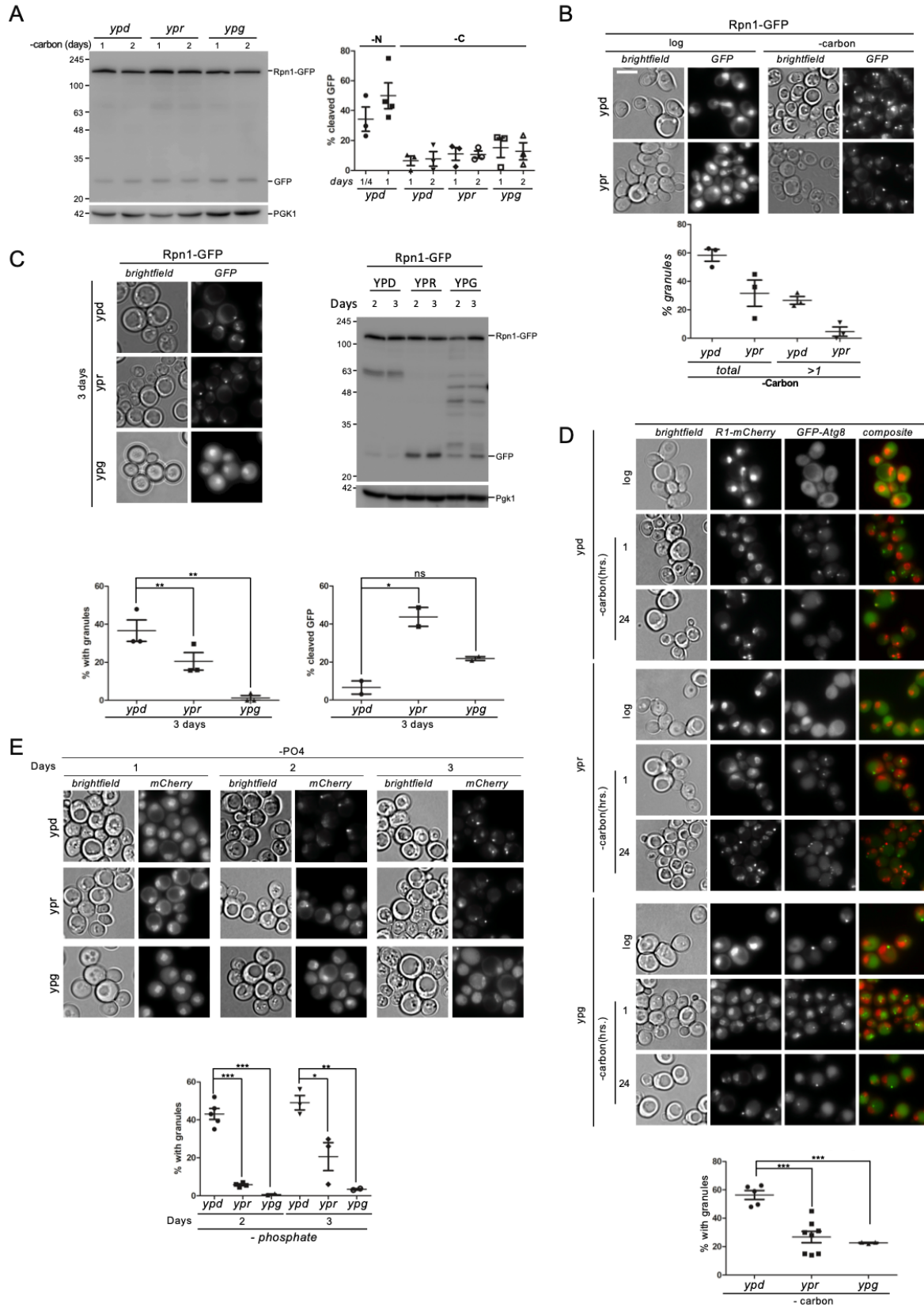
590 Supplementary information contains tables S1 and S2, supplementary figures S1-S12
591 and complete images of immunoblots used.

592

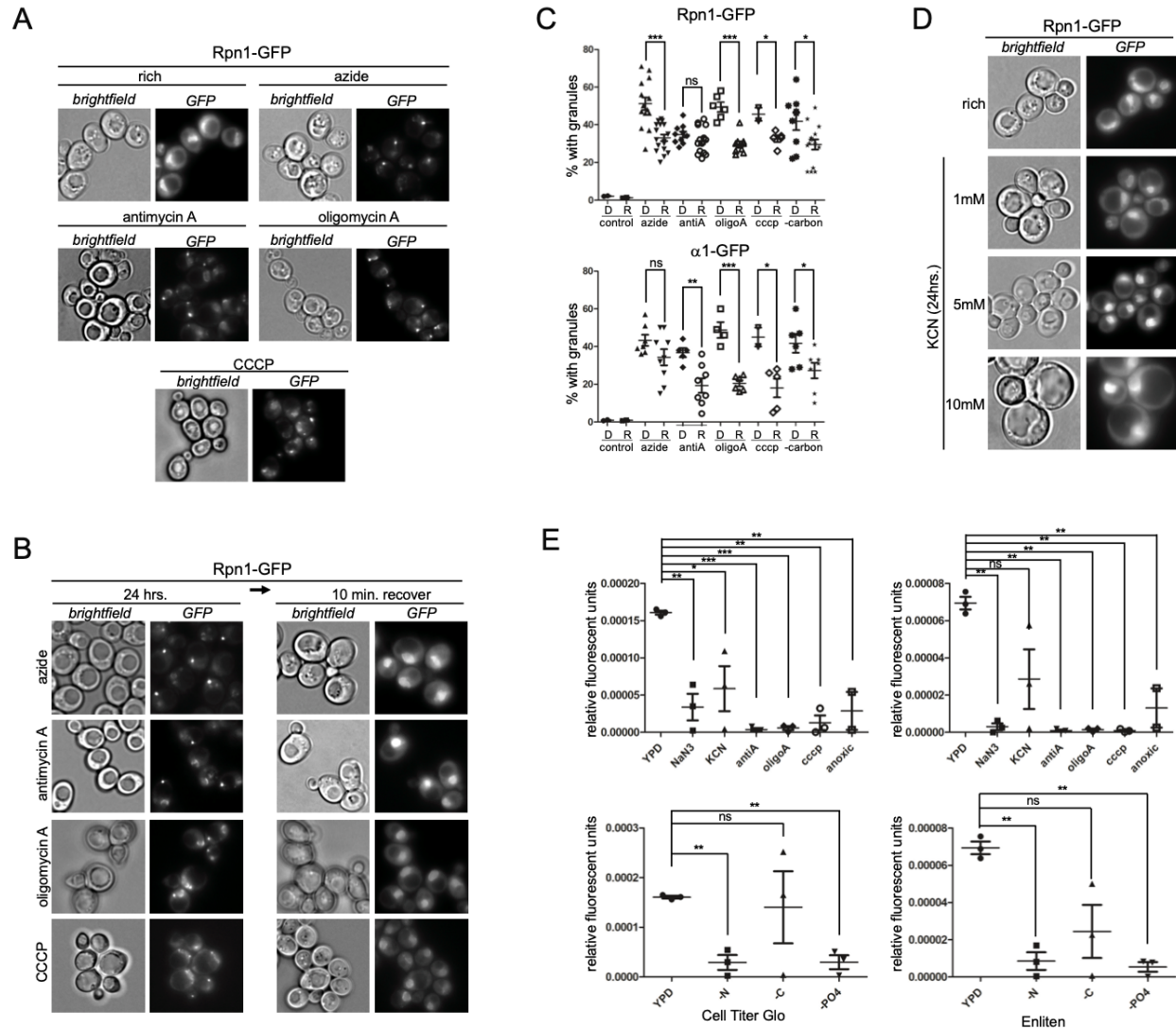
593

594

595 **Figures**



597 **Figure 1. Proteasome granule formation is restricted during respiratory growth. (A)** Rpn1-GFP expressing cells
598 were grown for four hours in rich media containing dextrose (ypd), raffinose (ypr) or glycerol (ypg), followed by
599 growth in SD media lacking carbon. 2 ODs of cells (i.e., the cells equivalent to two ml of culture OD₆₀₀ 1) were
600 harvested at indicated times and lysed as described in materials and methods. Lysates were separated by SDS-PAGE
601 and immunoblotted for GFP and Pgk1. Data presented are representative of three independent experiments.
602 Quantifications show the percentage of free GFP relative to the total amount of GFP (i.e., unprocessed + free GFP)
603 observed following nitrogen or carbon starvation. **(B)** Cells grown as in A were imaged at log phase and following 24
604 hours carbon starvation. Quantification shows the percentage of cells that induced proteasome granules and the percent
605 of those cells that formed two or more granules (Data presented are representative of three independent experiments
606 with n>100 for each). Scale bar represents 5 μ m. **(C)** (left) Rpn1-GFP expressing cells were grown for 3 days in the
607 indicated media then imaged microscopically. Quantification shows the percent of cells with granules from three
608 independent experiments. Statistical significance was determined with paired t-test (left) and n>100 for each datapoint.
609 (right) 2 ODs of cells were collected from cultures as in the left panel and lysed for immune blotting against GFP or
610 Pgk1. Data presented are representative of two independent experiments. Quantification shows the percentage of free
611 GFP, which indicating proteasome autophagy, relative to total GFP. Significance was determined using an unpaired
612 t-test. **(D)** Rpn1-mCherry (R1-mCherry); GFP-Atg8 expressing cells were grown in rich dextrose (ypd), raffinose
613 (ypr) or glycerol (ypg) media followed by a change to carbon starvation media. Microscopy was performed at indicated
614 times and quantifications show the percentage of cells with granules after 24 hours. Unpaired t-test was used to
615 determine significance and n>100 for each data point. **(E)** Rpn1-mCherry expressing yeast were grown in indicated
616 rich media for 4 hours, washed and switched to phosphate starvation media. Microscopy was performed at the
617 indicated times. Quantification shows the percent of cells that formed granules at 2 and 3 days of phosphate starvation.
618 Unpaired t-test was used to determine significance with n>100 for each datapoint.
619



620

621 **Figure 2. Mitochondrial inhibition induces proteasome granule formation.** (A) Rpn1-GFP expressing cells were

622 grown in rich media containing dextrose and treated with mitochondria inhibitors as described in materials and

623 methods. Microscopy was performed 24 hours after inhibitor addition. Data are representative of three independent

624 experiments. (B) Rpn1-GFP expressing cells treated for 24 hours with mitochondria inhibitors were washed and

625 incubated in drug free media for 10 minutes. Data are representative of three independent experiments. (C) Rpn1-GFP

626 or $\alpha 1$ -GFP expressing cells were grown in media containing dextrose (D) or raffinose (R) for 4 hours, treated with

627 mitochondria inhibitors, followed by and incubation for 24 hours. Microscopy was carried out and quantifications

628 show the percentage of cells with granules. Unpaired t-tests were used to determine significance with $n > 100$ for each

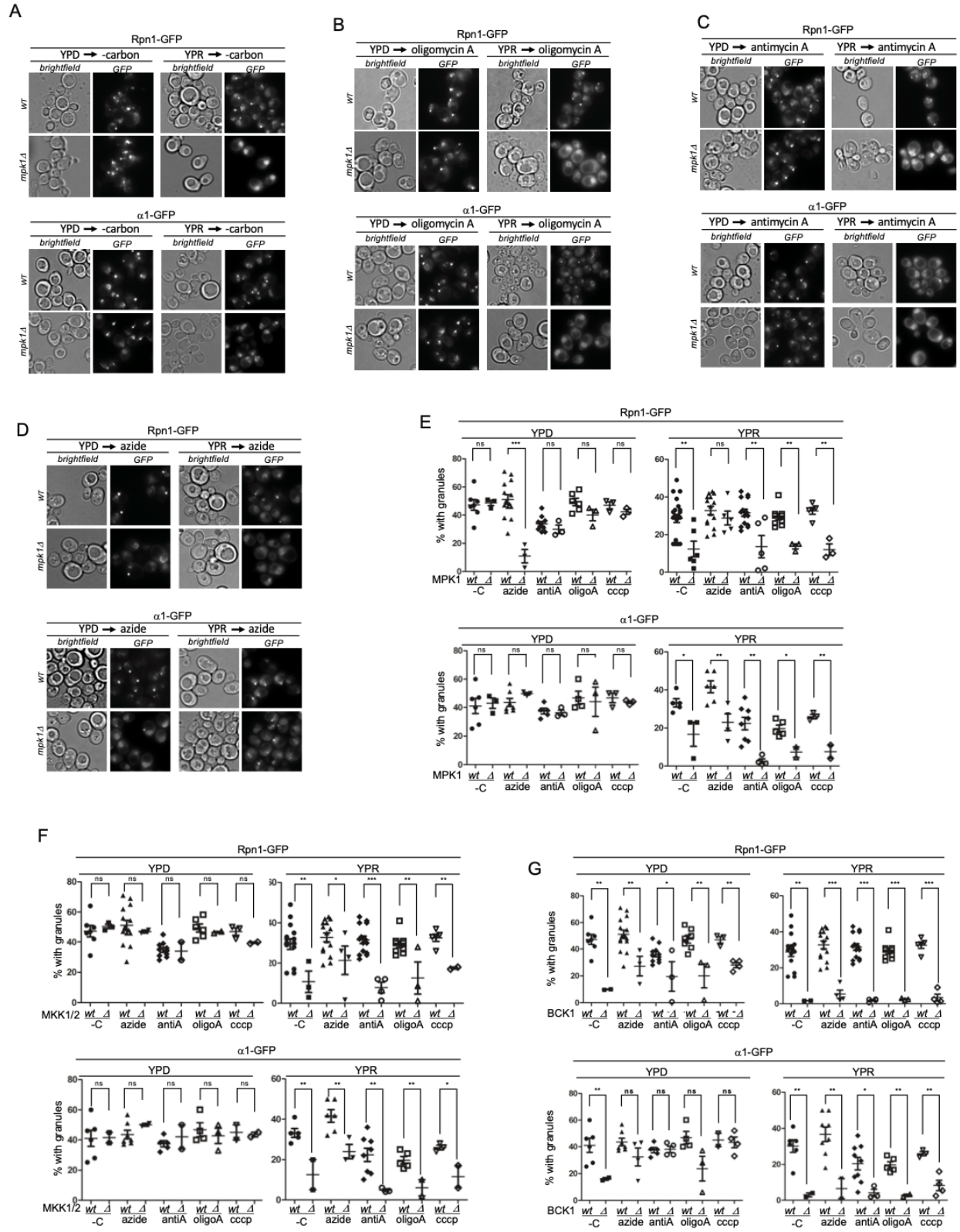
629 datapoint. (D) Yeast expressing Rpn1-GFP were treated with increasing concentrations of potassium cyanide for 24

630 hours followed by microscopic analysis. Data are representative of three independent experiments. (E) ATP

631 measurements were carried out following mitochondrial inhibition (upper panels) or nutrient starvation (lower panels)

632 as described in materials and methods. Quantifications show relative ATP compared to untreated controls averaged

633 from three independent experiments. Paired t-tests were used to evaluate significance.

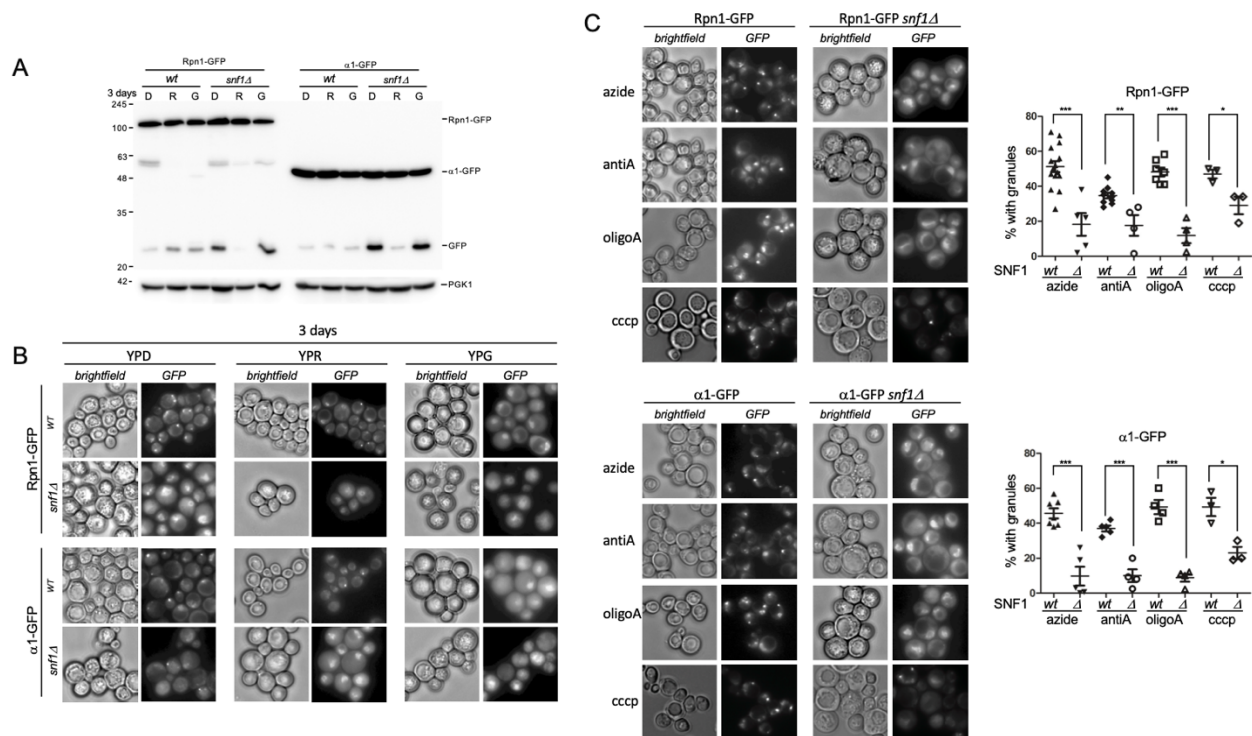


634

635

636 **Figure 3. MAP kinase signaling is required for proteasome granule formation. (A-D)** WT and *mpk1Δ* yeast
637 expressing Rpn1-GFP or α 1-GFP were grown to log phase in rich media containing dextrose or raffinose. Next, cells
638 were starved for carbon, or treated with oligomycin A, antimycin A, or sodium azide for 24 hours and imaged. **(E)**
639 Quantification of the percent of granule formation from yeast cultured and treated as in A-D, or CCCP. Statistical
640 significance was determined using unpaired t-tests. Three or more independent experiments were quantified with
641 $n > 100$ for each datapoint. **(F)** wild type (wt) and MKK1 MKK2 double deletion yeast (Δ) expressing Rpn1-GFP or
642 α 1-GFP were grown in dextrose or raffinose for four hours, starved for carbon or treated with mitochondria inhibitors
643 as above. Graphs show the percent of cells with granules after 24 hours with significance determined by unpaired t-
644 tests. At least three independent experiments were quantified with $n > 100$ for each datapoint. **(G)** wild type and
645 *bck1Δ* yeast expressing Rpn1-GFP or α 1-GFP were grown to log phase in rich media containing dextrose or raffinose
646 then starved for carbon or treated with mitochondria inhibitors as above. Quantifications show the percent of cells that
647 formed granules after 24 hours. Unpaired t-tests were used to determine significance. At least three independent
648 experiments were quantified with $n > 100$ for each datapoint.
649
650

651



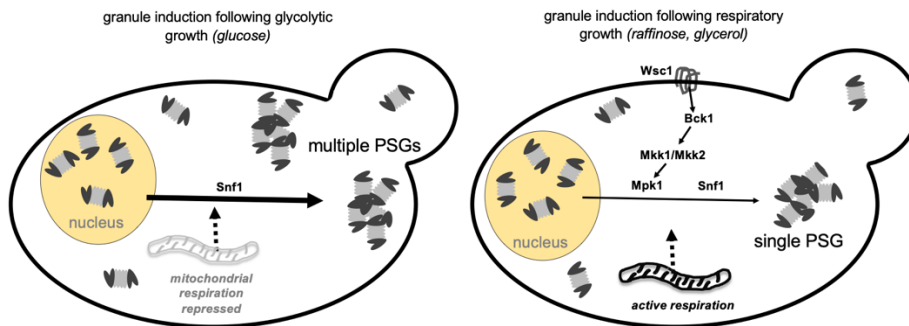
652

653

654 **Figure 4. Snf1 is required for proteasome granule formation upon mitochondrial inhibition.** (A) wild type (wt)
 655 and SNF1 deleted yeast expressing Rpn1-GFP or $\alpha 1$ -GFP were grown for three days in rich media containing dextrose,
 656 raffinose or glycerol (D, R and G respectively). Cells were harvested and lysed as described in materials and methods.
 657 Immune blotting for GFP and Pgk1 was performed. Data are representative of two independent experiments. (B) Cells
 658 from A were imaged microscopically to observe proteasome localization. Data are representative of two independent
 659 experiments. (C) Yeast as in A and B were grown in YPD medium to log phase and starved for carbon or treated with
 660 mitochondria inhibitors. Microscopy was performed and quantifications show the percent of cells that form granules
 661 following mitochondria inhibition in the SNF1 deleted yeast compared to wild type. Significance was determined
 662 using unpaired t-tests. At least three independent experiments with $n > 100$ for each datapoint, were used for
 663 quantification.

664

665



666

667

668 **Figure 5. Model for PSG formation following glycolytic or respiratory growth**

669 Switching from glycolytic growth media (i.e., with repressed mitochondrial respiration) to carbon starvation results
670 in the formation of multiple proteasome granules per cell and more proteasome granules as compared to cells starved
671 after growth in respiratory media. The kinase Snf1 is required for proteasome granule formation upon mitochondrial
672 inhibition but not carbon starvation. The cell integrity MAP kinase cascade (from Wsc1 to Mpk1) is required from
673 proteasome granule formation following respiratory but not glycolytic growth.

674

675

676 **References**

677

678 Adachi, A., Koizumi, M. and Ohsumi, Y. (2017) 'Autophagy induction under carbon starvation
679 conditions is negatively regulated by carbon catabolite repression.', *The Journal of biological*
680 *chemistry*. American Society for Biochemistry and Molecular Biology, 292(48), pp. 19905–19918.
681 doi: 10.1074/jbc.M117.817510.

682 Backhaus, K. *et al.* (2013) 'Mutations in SNF1 complex genes affect yeast cell wall strength',
683 *European Journal of Cell Biology*. doi: 10.1016/j.ejcb.2014.01.001.

684 BAO, W. *et al.* (2016) 'Induction of autophagy by the MG-132 proteasome inhibitor is associated
685 with endoplasmic reticulum stress in MCF-7 cells', *Molecular Medicine Reports*, 13(1), pp. 796–
686 804. doi: 10.3892/mmr.2015.4599.

687 Boos, F. *et al.* (2019) 'Mitochondrial protein-induced stress triggers a global adaptive
688 transcriptional programme', *Nature Cell Biology*. doi: 10.1038/s41556-019-0294-5.

689 Bragoszewski, P. *et al.* (2013) 'The ubiquitin-proteasome system regulates mitochondrial
690 intermembrane space proteins.', *Molecular and cellular biology*. American Society for

- 691 Microbiology (ASM), 33(11), pp. 2136–48. doi: 10.1128/MCB.01579-12.
- 692 Bragoszewski, P., Turek, M. and Chacinska, A. (2017) ‘Control of mitochondrial biogenesis and
693 function by the ubiquitin-proteasome system.’, *Open biology*. The Royal Society, 7(4). doi:
694 10.1098/rsob.170007.
- 695 Choi, W. H. *et al.* (2020) ‘Aggresomal sequestration and STUB1-mediated ubiquitylation during
696 mammalian proteophagy of inhibited proteasomes’, *Proceedings of the National Academy of
697 Sciences of the United States of America*. National Academy of Sciences, 117(32), pp. 19190–
698 19200. doi: 10.1073/pnas.1920327117.
- 699 Ciechanover, A. and Brundin, P. (2003) ‘The Ubiquitin Proteasome System in Neurodegenerative
700 Diseases’, *Neuron*. Elsevier, 40(2), pp. 427–446. doi: 10.1016/S0896-6273(03)00606-8.
- 701 Cohen-Kaplan, V. *et al.* (2016) ‘p62- and ubiquitin-dependent stress-induced autophagy of the
702 mammalian 26S proteasome.’, *Proceedings of the National Academy of Sciences of the United
703 States of America*. National Academy of Sciences, 113(47), pp. E7490–E7499. doi:
704 10.1073/pnas.1615455113.
- 705 Deffieu, M. *et al.* (2013) ‘Increased levels of reduced cytochrome b and mitophagy components
706 are required to trigger nonspecific autophagy following induced mitochondrial dysfunction’,
707 *Journal of Cell Science*, 126(2), pp. 415–426. doi: 10.1242/jcs.103713.
- 708 van Deventer, S. *et al.* (2014) ‘N-terminal acetylation and replicative age affect proteasome
709 localization and cell fitness during aging’, *Journal of Cell Science*, 128(1), pp. 109–117. doi:
710 10.1242/jcs.157354.
- 711 Dikic, I. (2017) ‘Proteasomal and Autophagic Degradation Systems’, *Annual Review of
712 Biochemistry*. Annual Reviews , 86(1), pp. 193–224. doi: 10.1146/annurev-biochem-061516-
713 044908.
- 714 Enenkel, C. (2012) ‘Using Native Gel Electrophoresis and Phosphofluoroimaging to Analyze
715 GFP-Tagged Proteasomes’, in. Humana Press, pp. 339–348. doi: 10.1007/978-1-61779-474-2_23.
- 716 Enenkel, C. (2018) ‘The paradox of proteasome granules’, *Current Genetics*, 64(1), pp. 137–140.
717 doi: 10.1007/s00294-017-0739-y.
- 718 Feng, Y. *et al.* (2014) ‘The machinery of macroautophagy.’, *Cell research*. Shanghai Institutes for
719 Biological Sciences, Chinese Academy of Sciences, 24(1), pp. 24–41. doi: 10.1038/cr.2013.168.
- 720 Finley, D. (2009) ‘Recognition and processing of ubiquitin-protein conjugates by the proteasome.’,
721 *Annual review of biochemistry*, 78, pp. 477–513. doi:

- 722 10.1146/annurev.biochem.78.081507.101607.
- 723 Finley, D. *et al.* (2012) ‘The ubiquitin-proteasome system of *Saccharomyces cerevisiae*’, *Genetics*,
724 192(October), pp. 319–360. doi: 10.1534/genetics.112.140467.
- 725 Finley, D., Özkaynak, E. and Varshavsky, A. (1987) ‘The yeast polyubiquitin gene is essential for
726 resistance to high temperatures, starvation, and other stresses’, *Cell*. Cell Press, 48(6), pp. 1035–
727 1046. doi: 10.1016/0092-8674(87)90711-2.
- 728 Fujii, K. *et al.* (2009) ‘A role for ubiquitin in the clearance of nonfunctional rRNAs’, *Genes &*
729 *Development*, 23(8), pp. 963–974. doi: 10.1101/gad.1775609.
- 730 Galdieri, L. *et al.* (2010) ‘Transcriptional regulation in yeast during diauxic shift and stationary
731 phase.’, *Omics : a journal of integrative biology*. Mary Ann Liebert, Inc., 14(6), pp. 629–38. doi:
732 10.1089/omi.2010.0069.
- 733 Goebel, T. *et al.* (2020) ‘Proteaphagy in mammalian cells can function independent of
734 ATG5/ATG7.’, *Molecular & cellular proteomics : MCP*. Mol Cell Proteomics. doi:
735 10.1074/mcp.RA120.001983.
- 736 Goldstein, A. L. and McCusker, J. H. (1999) ‘Three new dominant drug resistance cassettes for
737 gene disruption in *Saccharomyces cerevisiae*.’, *Yeast (Chichester, England)*, 15(14), pp. 1541–53.
738 doi: 10.1002/(SICI)1097-0061(199910)15:14<1541::AID-YEA476>3.0.CO;2-K.
- 739 Gribble, F. M. *et al.* (1997) ‘Properties of cloned ATP-sensitive K⁺ currents expressed in *Xenopus*
740 oocytes’, *Journal of Physiology*, 498(1). doi: 10.1113/jphysiol.1997.sp021843.
- 741 Gu, Z. C. *et al.* (2017) ‘Ubiquitin orchestrates proteasome dynamics between proliferation and
742 quiescence in yeast.’, *Molecular biology of the cell*. American Society for Cell Biology, 28(19),
743 pp. 2479–2491. doi: 10.1091/mbc.E17-03-0162.
- 744 Hailey, D. W., Davis, T. N. and Muller, E. G. D. (2002) ‘Fluorescence resonance energy transfer
745 using color variants of green fluorescent protein.’, *Methods in enzymology*, 351, pp. 34–49.
746 Available at: <http://www.ncbi.nlm.nih.gov/pubmed/12073355> (Accessed: 12 June 2019).
- 747 Hanssum, A. *et al.* (2014) ‘An Inducible Chaperone Adapts Proteasome Assembly to Stress’,
748 *Molecular Cell*. Cell Press, 55(4), pp. 566–577. doi: 10.1016/J.MOLCEL.2014.06.017.
- 749 Hershko, A. and Ciechanover, A. (1998) ‘The ubiquitin system.’, *Annual review of biochemistry*.
750 Annual Reviews 4139 El Camino Way, P.O. Box 10139, Palo Alto, CA 94303-0139, USA, 67,
751 pp. 425–79. doi: 10.1146/annurev.biochem.67.1.425.
- 752 Heytler, P. G. and Prichard, W. W. (1962) ‘A new class of uncoupling agents - Carbonyl cyanide

753 phenylhydrazones’, *Biochemical and Biophysical Research Communications*, 7(4). doi:
754 10.1016/0006-291X(62)90189-4.

755 Janke, C. *et al.* (2004) ‘A versatile toolbox for PCR-based tagging of yeast genes: new fluorescent
756 proteins, more markers and promoter substitution cassettes’, *Yeast*. John Wiley & Sons, Ltd,
757 21(11), pp. 947–962. doi: 10.1002/yea.1142.

758 Junn, E. *et al.* (2002) ‘Parkin accumulation in aggresomes due to proteasome impairment.’, *The*
759 *Journal of biological chemistry*. American Society for Biochemistry and Molecular Biology,
760 277(49), pp. 47870–7. doi: 10.1074/jbc.M203159200.

761 Kabeya, Y. *et al.* (2000) ‘LC3, a mammalian homologue of yeast Apg8p, is localized in
762 autophagosome membranes after processing.’, *The EMBO journal*. European Molecular Biology
763 Organization, 19(21), pp. 5720–8. doi: 10.1093/emboj/19.21.5720.

764 Kamada, Y. *et al.* (2010) ‘Tor Directly Controls the Atg1 Kinase Complex To Regulate
765 Autophagy’, *Molecular and Cellular Biology*, 30(4), pp. 1049–1058. doi: 10.1128/MCB.01344-
766 09.

767 Karmon, O. and Ben Aroya, S. (2020) ‘Spatial Organization of Proteasome Aggregates in the
768 Regulation of Proteasome Homeostasis’, *Frontiers in Molecular Biosciences*. doi:
769 10.3389/fmolb.2019.00150.

770 Kayikci, Ö. and Nielsen, J. (2015) ‘Glucose repression in *Saccharomyces cerevisiae*.’, *FEMS yeast*
771 *research*. Oxford University Press, 15(6). doi: 10.1093/femsyr/fov068.

772 Kleijnen, M. F. *et al.* (2007) ‘Stability of the proteasome can be regulated allosterically through
773 engagement of its proteolytic active sites’, *Nature Structural & Molecular Biology*, 14(12), pp.
774 1180–1188. doi: 10.1038/nsmb1335.

775 Ko, Y. H., Hong, S. and Pedersen, P. L. (1999) ‘Chemical mechanism of ATP synthase.
776 Magnesium plays a pivotal role in formation of the transition state where ATP is synthesized from
777 ADP and inorganic phosphate.’, *The Journal of biological chemistry*. American Society for
778 Biochemistry and Molecular Biology, 274(41), pp. 28853–6. doi: 10.1074/jbc.274.41.28853.

779 Kraft, C., Reggiori, F. and Peter, M. (2009) ‘Selective types of autophagy in yeast’, *Biochimica et*
780 *Biophysica Acta (BBA) - Molecular Cell Research*, 1793(9), pp. 1404–1412. doi:
781 10.1016/j.bbamcr.2009.02.006.

782 Krause, S. A., Xu, H. and Gray, J. V. (2008) ‘The synthetic genetic network around PKC1
783 identifies novel modulators and components of protein kinase C signaling in *Saccharomyces*

- 784 cerevisiae', *Eukaryotic Cell*, 7(11). doi: 10.1128/EC.00222-08.
- 785 Kuranda, K. *et al.* (2006) 'Investigating the caffeine effects in the yeast *Saccharomyces cerevisiae*
- 786 brings new insights into the connection between TOR, PKC and Ras/cAMP signalling pathways',
- 787 *Molecular Microbiology*, 61(5), pp. 1147–1166. doi: 10.1111/j.1365-2958.2006.05300.x.
- 788 Kushnirov, V. V. (2000) 'Rapid and reliable protein extraction from yeast', *Yeast*. Wiley-
- 789 Blackwell, 16(9), pp. 857–860. doi: 10.1002/1097-0061(20000630)16:9<857::AID-
- 790 YEA561>3.0.CO;2-B.
- 791 Lang, M. J. *et al.* (2014) 'Glucose starvation inhibits autophagy via vacuolar hydrolysis and
- 792 induces plasma membrane internalization by down-regulating recycling', *Journal of Biological*
- 793 *Chemistry*, 289, pp. 16736–16747. doi: 10.1074/jbc.M113.525782.
- 794 Laporte, D. *et al.* (2008) 'Reversible cytoplasmic localization of the proteasome in quiescent yeast
- 795 cells', *The Journal of Cell Biology*, 181(5), pp. 737–745. doi: 10.1083/jcb.200711154.
- 796 Lavie, J. *et al.* (2018) 'Ubiquitin-Dependent Degradation of Mitochondrial Proteins Regulates
- 797 Energy Metabolism In Brief', *CellReports*, 23, pp. 2852–2863. doi: 10.1016/j.celrep.2018.05.013.
- 798 Levin, D. E. (2005) 'Cell Wall Integrity Signaling in *Saccharomyces cerevisiae* ', *Microbiology*
- 799 *and Molecular Biology Reviews*, 69(2). doi: 10.1128/mmbr.69.2.262-291.2005.
- 800 Li, D. *et al.* (2015) 'A fluorescent tool set for yeast Atg proteins', *Autophagy*, 11(6), pp. 954–960.
- 801 doi: 10.1080/15548627.2015.1040971.
- 802 Li, J. *et al.* (2019) 'AMPK regulates ESCRT-dependent microautophagy of proteasomes
- 803 concomitant with proteasome storage granule assembly during glucose starvation', *PLOS*
- 804 *Genetics*. Edited by A. K. Hopper, 15(11), p. e1008387. doi: 10.1371/journal.pgen.1008387.
- 805 Li, W. *et al.* (2008) 'Genome-wide and functional annotation of human E3 ubiquitin ligases
- 806 identifies MULAN, a mitochondrial E3 that regulates the organelle's dynamics and signaling',
- 807 *PLoS ONE*, 3(1). doi: 10.1371/journal.pone.0001487.
- 808 Mao, K. *et al.* (2011) 'Two MAPK-signaling pathways are required for mitophagy in
- 809 *Saccharomyces cerevisiae*', *The Journal of Cell Biology*, 193(4), pp. 755–767. doi:
- 810 10.1083/jcb.201102092.
- 811 Marshall, R. S. *et al.* (2015) 'Autophagic Degradation of the 26S Proteasome Is Mediated by the
- 812 Dual ATG8/Ubiquitin Receptor RPN10 in Arabidopsis', *Molecular Cell*, 58, pp. 1053–1066. doi:
- 813 10.1016/j.molcel.2015.04.023.
- 814 Marshall, R. S., McLoughlin, F. and Vierstra, R. D. (2016) 'Autophagic Turnover of Inactive 26S

815 Proteasomes in Yeast Is Directed by the Ubiquitin Receptor Cue5 and the Hsp42 Chaperone', *Cell*
816 *Reports*. Cell Press, 16(6), pp. 1717–1732. doi: 10.1016/J.CELREP.2016.07.015.

817 Marshall, R. S. and Vierstra, R. D. (2018) 'Proteasome storage granules protect proteasomes from
818 autophagic degradation upon carbon starvation', *eLife*, 7. doi: 10.7554/eLife.34532.

819 May, A. I., Prescott, M. and Ohsumi, Y. (2020) 'Autophagy facilitates adaptation of budding yeast
820 to respiratory growth by recycling serine for one-carbon metabolism', *Nature Communications*,
821 11(1). doi: 10.1038/s41467-020-18805-x.

822 Mochida, K. *et al.* (2015) 'Receptor-mediated selective autophagy degrades the endoplasmic
823 reticulum and the nucleus', *Nature*, 522(7556), pp. 359–362. doi: 10.1038/nature14506.

824 Nemeč, A. A. *et al.* (2017) 'Autophagic clearance of proteasomes in yeast requires the conserved
825 sorting nexin Snx4.', *The Journal of biological chemistry*. American Society for Biochemistry and
826 Molecular Biology, 292(52), pp. 21466–21480. doi: 10.1074/jbc.M117.817999.

827 Nicastro, R. *et al.* (2015) 'Enhanced amino acid utilization sustains growth of cells lacking
828 Snf1/AMPK', *Biochimica et Biophysica Acta - Molecular Cell Research*, 1853(7). doi:
829 10.1016/j.bbamcr.2015.03.014.

830 Ogata, M. *et al.* (2006) 'Autophagy is activated for cell survival after endoplasmic reticulum
831 stress.', *Molecular and cellular biology*. American Society for Microbiology (ASM), 26(24), pp.
832 9220–31. doi: 10.1128/MCB.01453-06.

833 Peters, L. Z. *et al.* (2016) 'Proteasome storage granules are transiently associated with the insoluble
834 protein deposit in *Saccharomyces cerevisiae*', *Journal of Cell Science*, 129(6), pp. 1190–1197.
835 doi: 10.1242/jcs.179648.

836 Peters Lee Zeev, Z. *et al.* (2013) 'Formation and dissociation of proteasome storage granules are
837 regulated by cytosolic pH', *Journal of Cell Biology*, 201(5), pp. 663–671. doi:
838 10.1083/jcb.201211146.

839 Petti, A. A. *et al.* (2011) 'Survival of starving yeast is correlated with oxidative stress response
840 and nonrespiratory mitochondrial function', *Proceedings of the National Academy of Sciences*,
841 108(45), pp. E1089–E1098. doi: 10.1073/pnas.1101494108.

842 Rittinger, K. and Ikeda, F. (2017) 'Linear ubiquitin chains: enzymes, mechanisms and biology',
843 *Open Biology*, 7(4), p. 170026. doi: 10.1098/rsob.170026.

844 Rousseau, A. and Bertolotti, A. (2016) 'An evolutionarily conserved pathway controls proteasome
845 homeostasis.', *Nature*. Nature Publishing Group, 536(7615), pp. 184–189. doi:

846 10.1038/nature18943.

847 Schmidt, R. M. *et al.* (2019) ‘The proteasome biogenesis regulator Rpn4 cooperates with the
848 unfolded protein response to promote ER stress resistance’, *eLife*, 8. doi: 10.7554/eLife.43244.

849 Schrader, E. K., Harstad, K. G. and Matouschek, A. (2009) ‘Targeting proteins for degradation.’,
850 *Nature chemical biology*, 5(11), pp. 815–22. doi: 10.1038/nchembio.250.

851 Schüller, H. J. (2003) ‘Transcriptional control of nonfermentative metabolism in the yeast
852 *Saccharomyces cerevisiae*’, *Current Genetics*. doi: 10.1007/s00294-003-0381-8.

853 Secco, D. *et al.* (2012) ‘Phosphate homeostasis in the yeast *Saccharomyces cerevisiae*, the key role
854 of the SPX domain-containing proteins’, *FEBS Letters*. No longer published by Elsevier, 586(4),
855 pp. 289–295. doi: 10.1016/J.FEBSLET.2012.01.036.

856 Shaid, S. *et al.* (2013) ‘Ubiquitination and selective autophagy.’, *Cell death and differentiation*.
857 Nature Publishing Group, 20(1), pp. 21–30. doi: 10.1038/cdd.2012.72.

858 Sundin, B. A. *et al.* (2004) ‘Localization of proteins that are coordinately expressed with Cln2
859 during the cell cycle’, *Yeast*. John Wiley & Sons, Ltd, 21(9), pp. 793–800. doi: 10.1002/yea.1133.

860 Symersky, J. *et al.* (2012) ‘Oligomycin frames a common drug-binding site in the ATP synthase’,
861 *Proceedings of the National Academy of Sciences of the United States of America*, 109(35). doi:
862 10.1073/pnas.1207912109.

863 Takeshige, K. *et al.* (1992) ‘Autophagy in yeast demonstrated with proteinase-deficient mutants
864 and conditions for its induction’, *The Journal of Cell Biology*, 119(2), pp. 301–311. doi:
865 10.1083/jcb.119.2.301.

866 Turcotte, B. *et al.* (2010) ‘Transcriptional regulation of nonfermentable carbon utilization in
867 budding yeast’, *FEMS Yeast Research*. doi: 10.1111/j.1567-1364.2009.00555.x.

868 Um, J. W. *et al.* (2010) ‘Parkin directly modulates 26S proteasome activity.’, *The Journal of*
869 *neuroscience: the official journal of the Society for Neuroscience*. Society for Neuroscience,
870 30(35), pp. 11805–14. doi: 10.1523/JNEUROSCI.2862-09.2010.

871 Uriarte, M. *et al.* (2021) ‘Starvation-induced proteasome assemblies in the nucleus link amino acid
872 supply to apoptosis’, *Nature Communications*, 12(1). doi: 10.1038/s41467-021-27306-4.

873 Verna, J. *et al.* (1997) ‘A family of genes required for maintenance of cell wall integrity and for
874 the stress response in *Saccharomyces cerevisiae*’, *Proceedings of the National Academy of*
875 *Sciences of the United States of America*, 94(25). doi: 10.1073/pnas.94.25.13804.

876 Waite, K. A. *et al.* (2015) ‘Starvation Induces Proteasome Autophagy with Different Pathways for

877 Core and Regulatory Particle.’, *The Journal of biological chemistry*, p. M115.699124-. doi:
878 10.1074/jbc.M115.699124.

879 Waite, K. A. *et al.* (2016) ‘Starvation induces proteasome autophagy with different pathways for
880 core and regulatory particles’, *Journal of Biological Chemistry*, 291(7), pp. 3239–3253. doi:
881 10.1074/jbc.M115.699124.

882 Waite, K. A. *et al.* (2021) ‘Proteaphagy is specifically regulated and requires factors dispensable
883 for general autophagy’, *Journal of Biological Chemistry*, 298(1), p. 101494. doi:
884 10.1016/j.jbc.2021.101494.

885 Waite, K. A., Burris, A. and Roelofs, J. (2020) ‘Tagging the proteasome active site $\beta 5$ causes tag
886 specific phenotypes in yeast’, *Scientific Reports*, 10(1). doi: 10.1038/s41598-020-75126-1.

887 Webb, J. L. *et al.* (2003) ‘ α -Synuclein Is Degraded by Both Autophagy and the Proteasome’,
888 *Journal of Biological Chemistry*, 278(27), pp. 25009–25013. doi: 10.1074/jbc.M300227200.

889 Weberruss, M. H. *et al.* (2013) ‘Blm10 facilitates nuclear import of proteasome core particles.’,
890 *The EMBO journal*. European Molecular Biology Organization, 32(20), pp. 2697–707. doi:
891 10.1038/emboj.2013.192.

892 Wikström, M. K. F. and Berden, J. A. (1972) ‘Oxidoreduction of cytochrome b in the presence of
893 antimycin’, *BBA - Bioenergetics*, 283(3). doi: 10.1016/0005-2728(72)90258-7.

894 Willis, S. D. *et al.* (2018) ‘Snf1 cooperates with the CWI MAPK pathway to mediate the
895 degradation of Med13 following oxidative stress’, *Microbial Cell*. doi: 10.15698/mic2018.08.641.

896 Yasuda, S. *et al.* (2020) ‘Stress- and ubiquitylation-dependent phase separation of the proteasome’,
897 *Nature*, 578(7794). doi: 10.1038/s41586-020-1982-9.

898 Yi, C. *et al.* (2017) ‘Formation of a Snf1-Mec1-Atg1 Module on Mitochondria Governs Energy
899 Deprivation-Induced Autophagy by Regulating Mitochondrial Respiration’, *Developmental Cell*,
900 41(1), pp. 59-71.e4. doi: 10.1016/j.devcel.2017.03.007.

901